Growth and Device Application of CdSe Nanostructures

*Lijuan Zhao, Linfeng Hu, and Xiaosheng Fang**

Inorganic semiconductor nanostructures have attracted increasing interest in recent years because of their distinguishable role in fundamental studies and technical applications, mainly due to their size- and shape-dependent properties and flexible processing methods. The use of such nanostructures in optic, optoelectric, and piezoelectric prospects is expected to play a crucial role in future nanoscale devices. Cadmium selenide (CdSe), a well-known direct bandgap II-VI semiconductor in which the bandgap favors absorption over a wide range of the visible spectrum, has been a promising material for applications in such fields as photodetectors, field-effect transistors (FETs), field emitters, solar cells, light-emitting diodes (LEDs), memory devices, biosensors, and biomedical imaging. The research on CdSe nanostructures has made remarkable progress in the last few years. The research activities on CdSe nanostructures including various methods for the synthesis of CdSe nanostructures and the unique properties and device applications of these nanostructures are reviewed. Potential future directions of this research area are also highlighted.

1. Introduction

Cadmium selenide (CdSe), a of the well-known direct bandgap II-VI semiconductors, has been found in three crystalline forms: wurtzite (hexagonal), sphalerite (cubic, zinc blende), and rock-salt (cubic). The structure of sphalerite is unstable and converts to the wurtzite structure upon moderate heating, through a transition that starts at about 130 °C and is completed at about 700 °C within a day, while the rock-salt structure is only observed under high pressure.[1] CdSe has bandgap of ≈1.797 eV in the wurtzite crystal phase and ≈1.712 eV in the zinc blende phase.[2] Such a wide bandgap favors absorption over a wide range of the visible spectrum. Normally, CdSe is an n-type semiconductor. p-Type doping has been achieved by Ohtsuka and co-workers through the growth of p-type CdSe layers with zinc blende structure and a hole concentration of 1×10^{17} cm^{-3} using molecular beam epitaxy (MBE) with a nitrogen plasma source.[3]

Inorganic semiconductor nanostructures have exhibited interesting and novel size-dependent physical properties that differ greatly from those of the corresponding bulk materials due to the quantum confinement effect.[4–7] A representative example is quantum dots, which are matter (e.g., semiconductor) with excitons confined in all three spatial dimensions. The case of CdSe, the energy gap decreases as size increases from small quantum dots to large quantum dots and then to the bulk semiconductor. For example, a 2.4 nm-radius quantum dot has an energy gap of about 2 eV whereas a quantum dot of radius 0.9 nm has a gap of about 2.7 eV. Considering the Bohr exciton radius for CdSe (about 5.4 nm bulk), the emission of CdSe quantum dots can be tuned precisely from deep red to blue by a reduction in the dot radius from 5 nm to 0.7 nm under ultraviolet (UV) illumination.[8] The characteristics of semiconductor nanostructures, including their optical, electronic, and catalytic properties, are also shape-dependent.[9–11] For example, CdSe quantum rods reveal linearly polarized emission, which the corresponding quantum dots do not exhibit.[11] This can be attributed to the dimensional anisotropy of quantum rods. Inorganic semiconductor nanostructures are very promising materials in applications such as catalysis,[12] light-emitting diodes (LEDs),[13] solar cells,[14] and biological fluorescence labels[15,16] because of the continuous tunability of their optical and electronic properties by simply changing the physical size of the nanocrystals, along with their saturated color emission compared to organic molecules. Nanoscale chalcogenides have attracted considerable attention due to their remarkable properties and brilliant applications prospects.[17,18] In particular, CdSe nanocrystals have been proposed as working elements for nanotransistors,[19] electrochromic materials,[20] and charge-coupling devices.[21] CdSe nanowires[22] and nanotubes[23] have also been fabricated using electrochemical and chemical methods and may find use in fabricating optoelectronic devices, such as solar cells, where the power conversion efficiency of nanorods has been demonstrated to be higher than that of quantum dots.[14] CdSe/ZnS quantum dots with core/shell structure exhibit a lasing effect and can be used for fluoric immunoassays, biological imaging, and biosensors.[24]

To date, there have been many methods developed to synthesize CdSe nanostructures,[25] which provide a great opportunity for using such materials in ways that exploit their novel properties to optimize their potential applications. Here, a selection of recent work related to CdSe nanostructures is reviewed, with particular focus on their growth and device applications. We begin, a detailed introduction of various methods for the preparation of CdSe nanostructures is presented, then the recent

Dr. L. J. Zhao, Dr. L. F. Hu, Prof. X. S. Fang
Department of Materials Science
Fudan University
Shanghai 200433, P. R. China
E-mail: xshfang@fudan.edu.cn

DOI: 10.1002/adfm.201103088

efforts and great developments in exploiting the novel properties and device applications of CdSe nanostructures are discussed. Finally, the possible challenges and opportunities that researchers face in this field are proposed.

2. Growth of CdSe Nanostructures

In the past few years, semiconductor nanostructures have been prepared using a variety of physical and chemical methods. Some examples of physical processes, characterized by high-energy input, include molecular beam epitaxy (MBE) and metal-organic chemical vapor deposition (MOCVD) approaches to quantum wells and quantum dots[26–28] and vapor-liquid-solid (VLS) approaches to quantum wires.[29,30] High-temperature methods have also been applied to chemical routes, including particle growth in glasses[31,32] and the solvothermal method. In addition, the "soft" (low-energy input) chemical route, i.e., chemical colloidal route, was broadly applied to synthesize the II-VI semiconductor nanostructures. Traditionally, CdSe nanostructures have been prepared using hydrothermal/solvothermal techniques, electrochemical deposition processes, chemical vapor deposition (CVD) and physical vapor deposition (PVD) processes, and colloidal methods.

2.1. Hydrothermal/Solvothermal Technique

A hydrothermal/solvothermal process can be defined as "a chemical reaction in a closed system in the presence of a solvent (aqueous and non aqueous solution) at a temperature higher than that of the boiling point of such a solvent."[33] In the 1990s, Qian, Li, and co-workers developed a milder and more convenient synthetic route, a solvothermal route, to synthesize a series of 1D ME (M = Zn, Cd, E = S, Se) nanostructures at relatively low temperature.[34,35] They found that only in coordinating amine solvents, could CdE (E = S, Se) be prepared through the elemental reaction between cadmium and chalcogen at relatively low temperature. Several solvents were used, including deionized water.[36] When powders of the elements Se and Cd were used as Se and Cd sources, Li and co-workers found that the obtained products were CdSe only in strongly coordinating alkylamine solvents, such as diethylamine, ethylenediamine (en), pyridine, and 1,6-diaminohexane, which are strong donor ligands having N-chelation. It was found that the solvent plays key role in the morphology of CdSe nanostructures.[34,37] CdSe nanorods can be obtained when en was used as both solvent and template (**Figure 1**a), while pyridine or diethylamine leads to CdSe nanoparticles (Figure 1b). A solvent-coordinating molecular template (SCMT) mechanism was proposed, according to which en can bound to and combine with Cd^{2+} in a line due to its structure to form a complex of $[Cd(en)_2]^{2+}$. With the increase in the temperature, the stability of the complexes decreased. At elevated temperature, Se may connect the complexes to form 1D structure CdSe nanorods. However, in pyridine, which has a weaker N-donor but no line structure like en, the solvent molecules can also coordinate with Cd^{2+} to form complexes, but the stability of the complex is much lower than that of complex of $[Cd(en)_2]^{2+}$. Hence, the

Lijuan Zhao received her BS in physics from Nanjing University. In 2007, she obtained her PhD from the Hong Kong University of Science and Technology. She joined in Donghua University as a lecturer in 2008. She is currently a postdoctoral fellow in the Department of Materials Science, Fudan University. Her current research interests include synthesis, novel properties, and applications of semiconductor nanostructures, with a special focus on CdSe nano-tetrapod-based photovoltaic devices.

Linfeng Hu received his BS and MS in materials science and engineering from Huazhong University of Science and Technology and Tsinghua University, respectively. In 2010, he earned his PhD in materials science and engineering from the National Institute of Materials Science (NIMS), Japan. After finishing his doctorate work, he joined the department of materials science at Fudan University. His current research interests include in the synthesis, self-assembly, and construction of low-dimensional semiconductor nanostructures into functional thin films and nanodevices and their novel properties.

Xiaosheng Fang received his PhD from the Institute of Solid State Physics (ISSP), Chinese Academy of Sciences (CAS) in 2006 under the supervision of Prof. Lide Zhang. He joined NIMS, Japan as a postdoctoral fellow and then the International Center for Young Scientists (ICYS)-International Center for Materials Nanoarchitectonics (MANA) as a researcher. Currently, he is a professor in the department of materials science at Fudan University (China). His current research topic is the controlled fabrication, novel properties, and optoelectronic applications of semiconductor nanostructures, with a particular focus on II-VI inorganic semiconductor nanostructure-based optoelectronic devices.

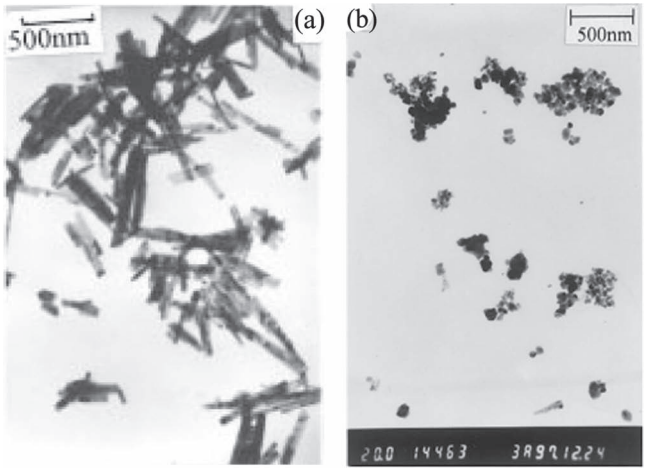

Figure 1. Hydrothermal/solvothermal synthesis of CdSe nanostructures in different solvents. a) CdSe nanorods prepared in en. Reproduced with permission.[37] Copyright 1999, American Chemical Society. b) TEM image of CdSe nanoparticles prepared in diethylamine. Reproduced with permission.[34] Copyright 1999, Elsevier Ltd.

epitaxial growth is difficult to realize, which induces the spherical morphology of CdSe.[37]

Peng and co-workers successfully synthesized wurtzite CdSe nanocrystals in a $NH_3 \cdot H_2O$ complexation system using $Cd(NO_3)_2 \cdot 4H_2O$, $NaSeO_3$, and $N_2H_4 \cdot H_2O$ as reactants. Zinc blende CdSe nanocrystals can be obtained only by changing the complexing agents from $NH_3 \cdot H_2O$ to ethylenediaminetetraacetic acid (EDTA) in NaOH solution.[38] They also found that the reaction temperature and Cd/Se ratio in the raw materials were important parameters influencing the morphologies and phases of the products. **Figure 2** shows the transmission electron microscopy (TEM) images of a series of CdSe nanocrystals with different morphologies obtained by altering the reaction conditions. The phase and morphologies of the CdSe nanocrystals can be readily controlled using this method. However, the reactant $NaSeO_3$ is highly toxic. In 2007, Lai and co-workers use Se powder, which is much less toxic than $NaSeO_3$, as the Se source and en as the solvent to synthesize CdSe nanostructures.[39] It was found that not only the structure, but also the morphology, of CdSe nanocrystals can be successfully tuned by changing the reactants' compositions. The amount and gain rate of Se^{2-} ions were found to be the decisive factor in determining the process of the reaction.

Gautam and co-workers reported a convenient and safe one-pot route to capped, large quantities of 3 nm zinc blende CdSe nanoparticles with a narrow size distribution that makes use of common starting materials and inexpensive, low-boiling point solvents under solvothermal conditions.[40a] Wang and co-workers used a solvothermal method to successfully synthesize zinc blende CdSe hollow nanospheres from the reaction of $Cd(NO_3)_2 \cdot 4H_2O$ with a homogeneously secondary Se source, which was first prepared by dissolving Se powder in a mixture of ethanol and oleic acid at 205 °C (**Figure 3**a). As Se powder directly reacted with $Cd(NO_3)_2 \cdot 4H_2O$ in the above mixed solvents, wurtzite CdSe solid nanoparticles were produced (Figure 3b).[40b]

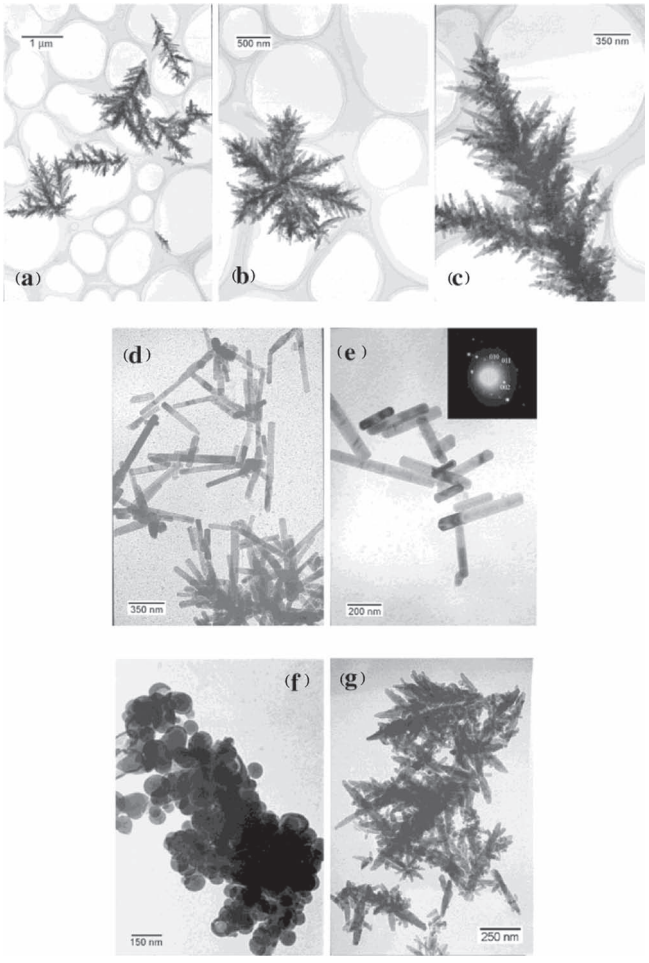

Figure 2. TEM images of CdSe fractals, nanorods, and other morphologies prepared under different conditions: a–c) dendritic CdSe fractals at 100 °C in $NH_3 \cdot H_2O$ complexation system; d,e) CdSe nanorods at 180 °C in $NH_3 \cdot H_2O$ complexation system; f) CdSe spheres without using any complexing agent; and g) irregular branchlike CdSe nanocrystals as the Cd/Se ratio of raw materials was 1:1. Reproduced with permission.[38] Copyright 2002, American Chemical Society.

2.2. Electrochemical Deposition Process

Because the growth is controllable almost exclusively in the direction normal to the substrate surface, electrochemical synthesis in a template is taken as one of the most efficient methods to control the growth of nanowires.[41,42] In 2000, Xu and co-workers reported their work on fabricating CdSe nanowire arrays by direct-current (dc) electrodeposition in porous anodic aluminum oxide (AAO) templates from a dimethyl sulfoxide solution containing $CdCl_2$ and elemental Se (**Figure 4**).[43] These nanowires have a hexagonal phase determined by X-ray diffraction (XRD) and have uniform diameters of about 20 nm, which corresponds closely to the pore diameters.

Su and co-workers used electron-beam (E-beam) lithography and electrochemical deposition to fabricate 2D arrays of CdSe pillars with a large height-to-width ratio.[44] The minimum pillar diameter was about 80 nm and the height of the tallest pillar was about 640 nm. Depositing CdSe pillars to a height over that

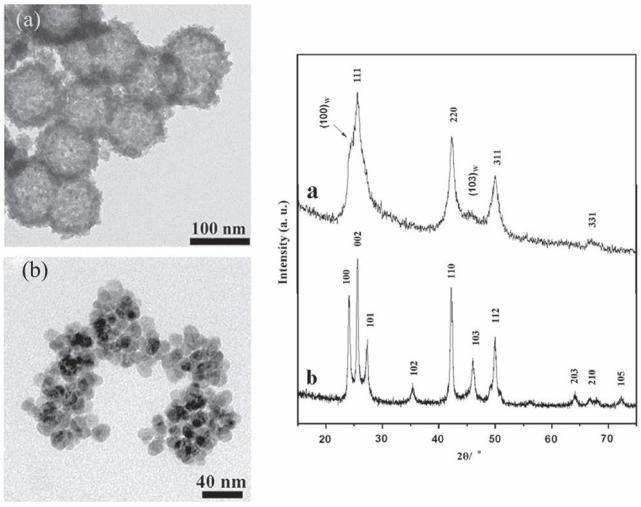

Figure 3. TEM images and XRD patterns of a) CdSe hollow nanostructures and b) CdSe solid nanoparticles. Reproduced with permission.[40b] Copyright 2010, Elsevier Ltd.

of the resist results in mushroom structures. **Figure 5**a,b show typical scanning electron microscopy (SEM) images of the pillar arrays and mushroom-like pillar arrays, respectively. These arrays should have potential in optical devices applications such as filters, waveguides, cavity resonators, and photonic crystals.

2.3. Vapor Deposition Processes

Vapor deposition processes include PVD and CVD processes. There are few reports on the synthesis of CdSe nanostructures using PVD or CVD processes, but these nanostructures often have novel morphologies.

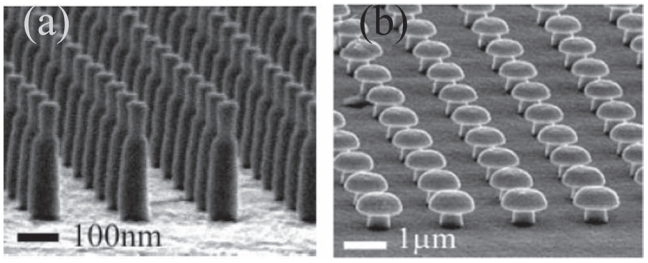

Figure 5. SEM images of CdSe a) pillars and b) mushroom-like pillars arrays made on indium tin oxide (ITO)/glass substrates. Reproduced with permission.[44]

Wang and co-workers use CdSe powder to fabricate CdSe nanobelts and nanosaws using a PVD process.[45a] The pure CdSe powder was evaporated at 750 °C under nitrogen gas, which acted as a carrier gas to transport the sublimated vapor to cooler regions for deposition. Single-crystal silicon substrates, dispersed with gold particles of typical sizes 3–5 nm that acted as catalyst were used to grow the nanostructure. **Figure 6** shows the as-grown CdSe nanostructures. The most dominant morphology is the saw-shaped nanoribbon (Figure 6a), with one side flat and one side with sharp "teeth". Nanobelts of CdSe are also found, but they are not the dominant component (Figure 6b). Subsequently, the authors carried out a systematic study on the growth of CdSe nanowires, nanobelts, and nanosaws using a Au-catalyzed VLS process and varying five different source temperatures and nine pressure settings, which yielded a total of 45 distinct experimental sets. For 150 experiments, they discussed the relationship between CdSe nanostructure morphology and the experimental pressure/temperature used and defined a road map to guide the synthesis of various CdSe nanostrctures.[45b]

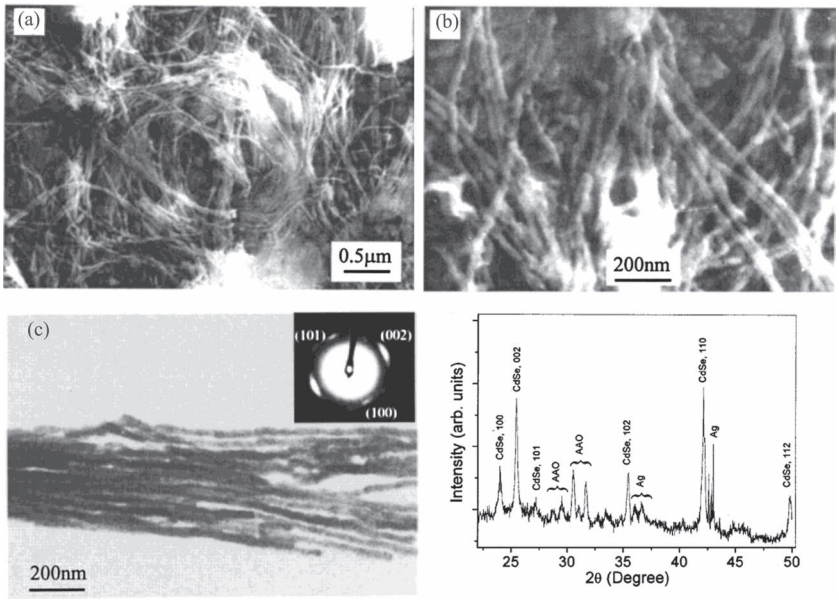

Figure 4. a,b) SEM and c) TEM images and XRD pattern of CdSe nanowire arrays. The electron diffraction (inset in (c)) and XRD patterns indicate the hexagonal CdSe crystal structure. Reproduced with permission.[43] Copyright 2000, American Chemical Society.

Single-crystalline CdSe nanobelts and nanosheets were synthesized using a CVD method assisted with laser ablation by Venugopal and co-workers.[46a] High-purity CdSe powder was used as source materials. A Si wafer coated with gold nanoparticles, which acted as the catalyst, was used as the collection substrate. The carrier gas was a mixture of Ar (90%) and H_2 (10%). When the gas flow became steady, a pulsed neodymium-doped yttrium aluminium garnet (Nd:YAG) laser with a 1064 nm wavelength was ignited to ablate the CdSe target. It was found that various morphological CdSe nanostructures were obtained at distinct deposition temperatures. The hexagonal-structure belts were generated with a high product yield at the deposition sites at 500–600 °C (**Figure 7**a). A typical TEM image for a single CdSe belt with a tapered width is depicted in Figure 7b. Most of the belt can range in tapered width and was about 3 μm at one end and tapered about 100 nm at a catalytic particle. At 650–700 °C, the

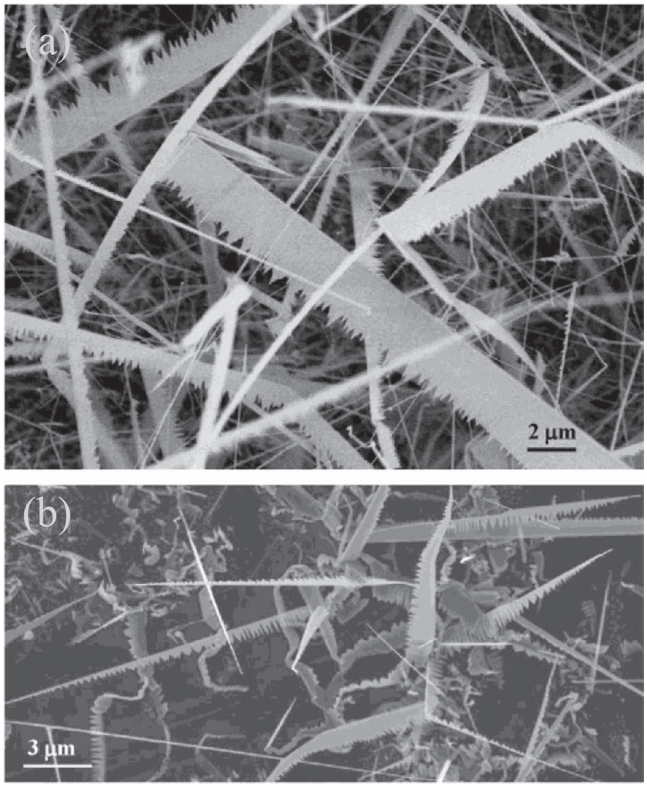

Figure 6. SEM images of CdSe nanosaws. Nanobelts were observed in (b), but they are not the dominant component. Reproduced with permission.[45a] Copyright 2004, American Chemical Society.

synthesized CdSe nanostructures have sheet-like morphology (Figure 7c). The as-synthesized sheets also have hexagonal wurtzite structure. Figure 7d shows a typical TEM image of a single CdSe sheet. The width of these sheets ranges from 2 μm to 5 μm, while the thickness is about 40–50 nm. Zhang and co-workers reported the growth of CdSe naowires, nanorods, nanoparticles, and tetrapod crystals using a Si-assisted CVD process. The as-synthesized morphologies of CdSe nanostructures can be controlled by manipulating the growth driving force, which promotes the degree of vapor supersaturation.[46b] The wurtzite CdSe tetrapods with hollow arms were synthesized using a simple CVD route in which Si powder and the mixture of the pure cadmium Cd and the pure Se powder were used as source materials.[46c]

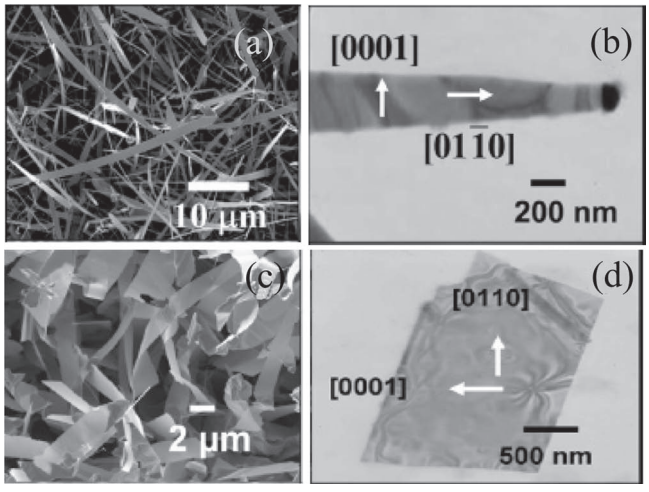

Figure 7. SEM and TEM images of as-synthesized CdSe: a,b) nanobelts and c,d) nanosheets. Reproduced with permission.[46a] Copyright 2005, American Chemical Society.

2.4. Colloidal Method

Colloidal semiconductor nanostructures have been widely investigated in recent years because the morphologies and sizes of such nanostructures can be more readily controlled. As a breakthrough in this field, Alivisatos, Peng, and co-workers synthesized a series of nearly monodispersed II-VI group nano-semiconductors using different cadmium precursors in trioctylphosphine oxide (TOPO).[47,48] They observed the nucleation and growth of these nanostructures and successfully controlled the morphology of the nanocrystals, from quantum dots to quantum rods. Using a colloidal method, the sizes of the resulting CdSe nanocrystals can be precisely controlled from several nanometers to tens of nanometers.

Alivisatos and co-workers used dimethylcadmium ($Cd(CH_3)_2$) and Se powder as the Cd and Se precursors, respectively, to synthesize CdSe nanorods.[47] The precursors were dissolved in tri-*n*-butylphosphine (TBP). In a typical synthesis, a mixture of hexylphosphonic acid (HPA), tetradecylphosphonic acid (TDPA), and TOPO was degassed at 120 °C for 1 h, after which the cadmium precursor solution was added dropwise. The resulting mixture was then heated to 360 °C and the Se precursor solution was quickly injected. After injection, the temperature dropped to 290 °C and was maintained at this level throughout the synthesis. By varying the relative concentration of TOPO:HPA:TDPA and the growth time, CdSe nanorods of different lengths and aspect ratios can be obtained. **Figure 8** shows TEM images of the as-prepared CdSe nanorods with different length.

Peng and co-workers have studied the shape-controlled CdSe nanocrystals via alternative routes.[48] Non-organic CdO, which is less toxic than dimethylcadmium, and Se powder were used as Cd and Se sources, respectively. TOPO and TDPA or

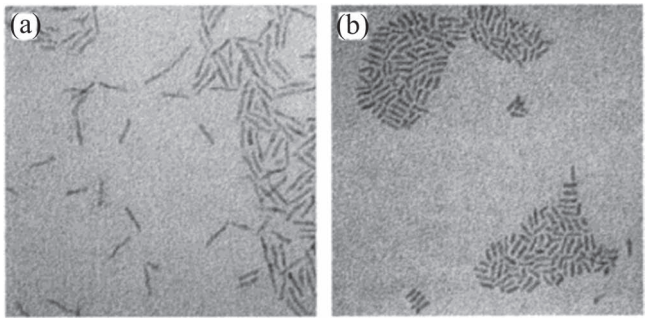

Figure 8. TEM images of as-prepared CdSe nanorods with a) medium and b) short length, respectively. Reproduced with permission.[47] Copyright 2002, American Chemical Society.

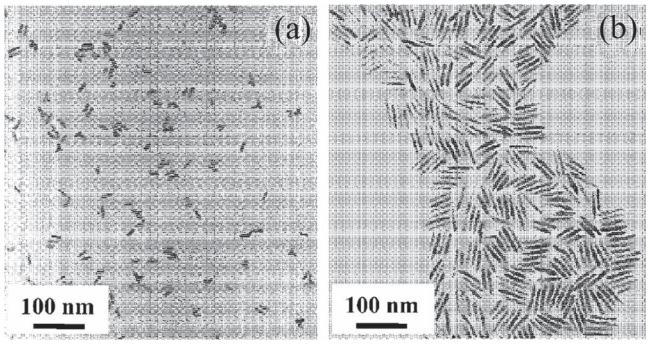

Figure 9. Influence of the history of Cd-TDPA complexes. a) Without aging at room temperature and b) aged at room temperature. Reproduced with permission.[48] Copyright 2002, American Chemical Society.

octadecyl phosphine acid (ODPA) were added to act as a coordinated surfactant and TOP was used as solvent for Se. They observed that the history of cadmium precursors had a noticeable effect on the aspect ratio of the resulting CdSe nanorods. When the Cd-TDPA-TOPO precursor was not aged at room temperature, the highest aspect ratio of the rods was about three (**Figure 9**a). The highest average aspect ratio of the resulting nanocrystals was about 6.5 when the cadmium precursor was aged at room temperature (Figure 9b). The monomer concentration also has large influence on the morphologies of CdSe nanocrystals. It was difficult to completely exclude the branched or multiarmed nanocryatals for the growth of rods. In contrast, branched structures were not observed in the cases of the formation of dot-shaped nanocrystals, which occurred at relatively low monomer concentrations. **Figure 10** reveals that the formation of branched nanocrystals was directly determined by the monomer concentration in the solution. By simply increasing the precursor concentration at 300 °C, the morphology of CdSe nanocrystals varied from short rods to long rods and then to branched ones.

High-yield CdSe nano-tetrapods could be obtained when oleic acid (OA) was used as the surfactant and proton acid was added to the cadmium precursor at relatively low reaction temperature (180 °C).[49] It was found that the resulting products were spherical CdSe nanocrystals when no proton acid was added. **Figure 11** shows the TEM images of the resulting spherical CdSe nanocrystals and high-yield CdSe nano-tetrapods by adding HCl. It was believed that the proton (H^+) plays a key role in the formation of the almost pure CdSe tetrapods.

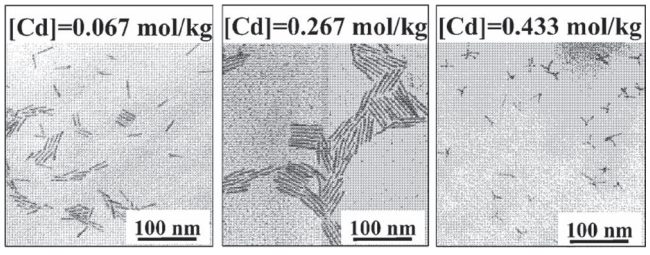

Figure 10. Monomer concentration dependence of the shape of CdSe grown at 300 °C with a Cd-ODPA complex as the cadmium precurcsor. Reproduced with permission.[48] Copyright 2002, American Chemical Society.

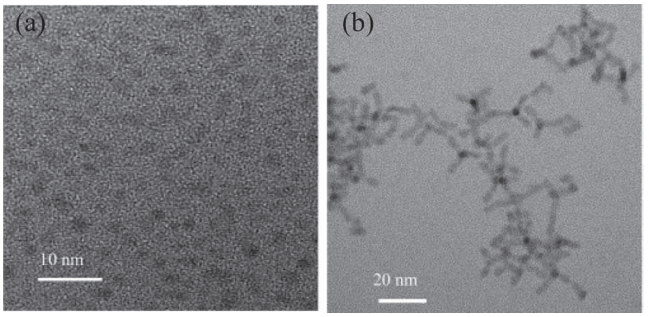

Figure 11. a) CdSe spherical and b) tetrapod-shaped nanocrystals prepared using a colloidal method. Reproduced with permission.[49] Copyright 2005, American Chemical Society.

2.5. Other Methods

A so-called "solution-liquid-solid" growth method was used to synthesize CdSe quantum wires.[50] These wires were prepared from cadmium stearate and n-R_3PSe (R = butyl or octyl) in TOPO at 240–300 °C using monodisperse Bi nanoparticles to catalyze wire growth. By varying the reaction temperature and the catalyst nanoparticle size, the wire diameters were controlled. The diameters of the resulting wires ranged from 5 to 20 nm, while the lengths of these wires were about several micrometers, as shown in **Figure 12**a.

Chen and co-workers successfully converted CdO into laminar wurtzite CdSe nanocrystals in a mixture of ethylenediamine and hydrazine hydrate at room temperature.[51] In a typical procedure, CdO and Se powder were added into the mixture of ethylenediamine and hydrazine hydrate, and the mixture was then vigorously stirred for 48 h at room temperature. After being washed by distilled water and absolute ethanol and dried, the precipitates were re-dispersed in HCl solution and stirred for 2 h. The final products were obtained after washing and drying. TEM images indicated that laminar CdSe nanocrystals were achieved through protonization of the complex (Figure 12b). Each of these nanocrystals is a well-crystallized CdSe nanocrystal according the discrete selected area electron diffraction (SAED) patterns as showed in the inset of Figure 12b.

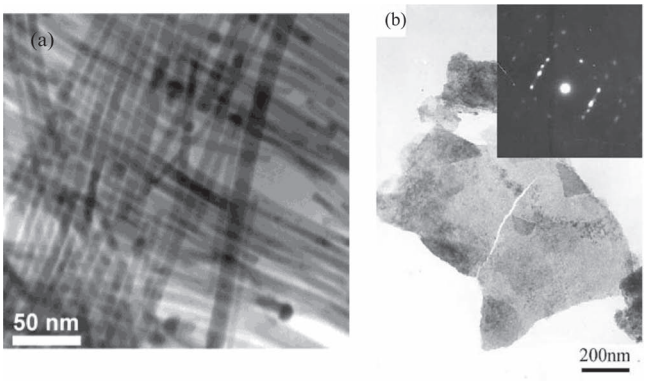

Figure 12. a) CdSe nanowires prepared by the solution-liquid-solid growth method. Reproduced with permission.[50] Copyright 2003, American Chemical Society. b) Laminar CdSe nanocrystals prepared at room temperature. Reproduced with permission.[51] Copyright 2004, Elsevier Ltd.

3. Novel Properties and Applications of CdSe

As an important II-VI semiconductor, CdSe nanostructures have attracted considerable attention due to its unique properties, which include a direct bandgap and excellent photoelectrical characteristics and make it a promising material for applications in many fields, such as photodetectors, FETs, field emitters, solar cells, LEDs, memory devices, biosensors, and biomedical imaging.

3.1. Photodetectors

Photodetectors are very important optoelectronic devices for practical applications involving photon detection in the visible light or ultraviolet region, which show widespread applications including environmental and biological research, sensors, missile launch, and light-wave communications. Generally, the key sensing element of a photodetector is made of semiconductor materials. Due to its photoconductive properties, the semiconductor shows sensitivity to the light that has a photon energy above its bandgap (E_g) and can be utilized in photon detection.[52]

With a direct bandgap, CdSe nanostructures have been exploited as a promising material for photodetectors. There have been a number of recent reports on optoelectronic properties of CdSe nanostructures. For example, Lee and co-workers synthesized CdSe nanoribbons using a thermal evaporation process in a horizontal quartz tube (as shown in **Figure 13**a).[53b] Then a photodetector was successfully constructed from an individual CdSe nanoribbon (illustrated in the inset in Figure 13b). Figure 13b presents the incident wavelength-dependent current–voltage (I–V) curves obtained when the CdSe nanoribbon was exposed to light of a different wavelength at an intensity of 4.10 mW cm^{-2}. The photoconductances of the CdSe nanoribbon are calculated to be 2816 nS at 650 nm and 0.095 nS in a dark state from the I–V curves. A cut-off wavelength of about 710 nm (closed to the CdSe bandgap emission) indicates the very low photosensitivity of the intrinsic CdSe nanoribbons when the wavelengths are longer than 710 nm. The photoconductance of the CdSe nanoribbion at 650 nm is approximately five orders of magnitude larger than that of the dark state, indicating the high light-sensitivity of the CdSe nanoribbon. The reversible switching behavior of the CdSe nanoribbon-based device when the light was turned off and on is shown in Figure 13c, and the device is found to work with excellent stability and reproducibility. These findings demonstrate the great potential for the use of CdSe nanoribbons in high-sensitivity photodetectors and photoelectronic switches. Based on this work, the authors also studied the photoelectrical properties of n-type CdSe nanowires with indium doping.[54] It was found that indium doping leads to significant improvements in the photoelectrical performance. Dai and co-workers also measured the impurity-dependent optoelectronic properties of CdSe nanobelts.[55] They found that intrinsic CdSe nanobelts are more suitable for fast and sensitive photodetector applications, while n-type CdSe nanobelts are more advantageous for high-gain photodetector applications. The different photoresponse properties result mainly from the impurity induced traps inside the CdSe nanobelts. Yun and co-workers decorated CdSe nanocrystals on single-walled carbon nanotubes by combining a method of chemically modified substrate, exhibiting a clear spectral response and photocurrent response.[56] Penner and co-workers recently developed the lithographically patterned nanowire electrodeposition (LPNE) method to prepare nanocrystalline CdSe (nc-CdSe) nanowires as shown in Figure 13d.[57,58] Lengths (5 μm) of these nanowires were electrically contacted by evaporated gold electrodes with a thickness of 40 nm to form an nc-CdSe nanowire array photodetector (Figure 13e). The photoconductivity of arrays of 350 CdSe nanowires is characterized by photosensitivity factors of 10–100 in addition to ultrafast response and recovery times of 20–40 μs (Figure 13f,g). This response speed is significantly shorter than that observed for all other nanowire systems to date. Most recently, they successfully optimized the performance of these nanomaterials as a function of the mean grain diameter.[59]

3.2. Field-Effect Transistors (FETs)

As a basic functional component in integrated circuits, displays, and memory devices, FETs play a core role in current electronic industry. The FETs based on individual nanostructure are regarded as a promising candidate for scaling down complementary metal-oxide-semiconductor (CMOS) devices. Since both the Hall and field-effect mobilities of CdSe (up to 800 cm^2 V^{-1} S^{-1}) substantially exceed those of Si, CdSe is a promising candidate semiconductor for inorganic FETs.[60] Recently, enormous effort has been devoted to exploring various FETs devices fabricated from CdSe nanostrcutures.[61,62] Lee and co-workers fabricated FET devices from an individual CdSe nanoribbon, showing a pronounced gating effect. The gate-dependent I_{ds}–V_{ds} characteristics reveal the n-type conductivity of CdSe, which most likely results from the selenium vacancies in CdSe. They further demonstrates the tuning of the electrical properties of CdSe nanowires by indium doping and construct FETs based on single CdSe:In nanowires.[54,63] The conductivity of CdSe nanowires was increased by nearly five orders of magnitude from ≈10^{-4} to tens of S cm^{-1} via doping and a carrier concentration as high as ≈10^{19} cm^{-3} was achieved for the heaviest doping.[53a] Marks and co-workers reported the first fabrication of thin-film-based FETs from solution-processed CdSe and a self-assembled nanodielectric (SAND) gate insulator composed of alkyl, siloxane, and stilbazolium layers.[64] In their study, CdSe thin films were grown using the chemical bath deposition (CBD) method using aqueous Cd^{2+} and sodium selenosulfate ($SeSO_3^{2-}$) solutions, and then bottom-gate/top-contact CdSe-based FETs were fabricated on both commercial n$^+$-Si/(16.5 nm) SAND substrates following identical CBD procedures for CdSe film growth. After annealing the films at 400 °C, the corresponding atomic force microscopy (AFM) image confirms the polycrystalline nature with a thickness of about 200 nm (see **Figure 14**a). FETs fabrication was completed by thermal evaporation of Au source and drain contacts (50 nm) through a shadow mask (see Figure 14b). Device parameters were then extracted from I–V plots as shown in Figure 14c. Figure 14d shows the average capacitance of CdSe film FET versus annealing temperature. Typical patterned SAND/CdSe devices exhibit an average field-effect mobility, μ_{FET} = 41 ± 15 cm^2 V^{-1} S^{-1} with a maximum observed μ_{FET} of ≈57 cm^2 V^{-1} S^{-1}.

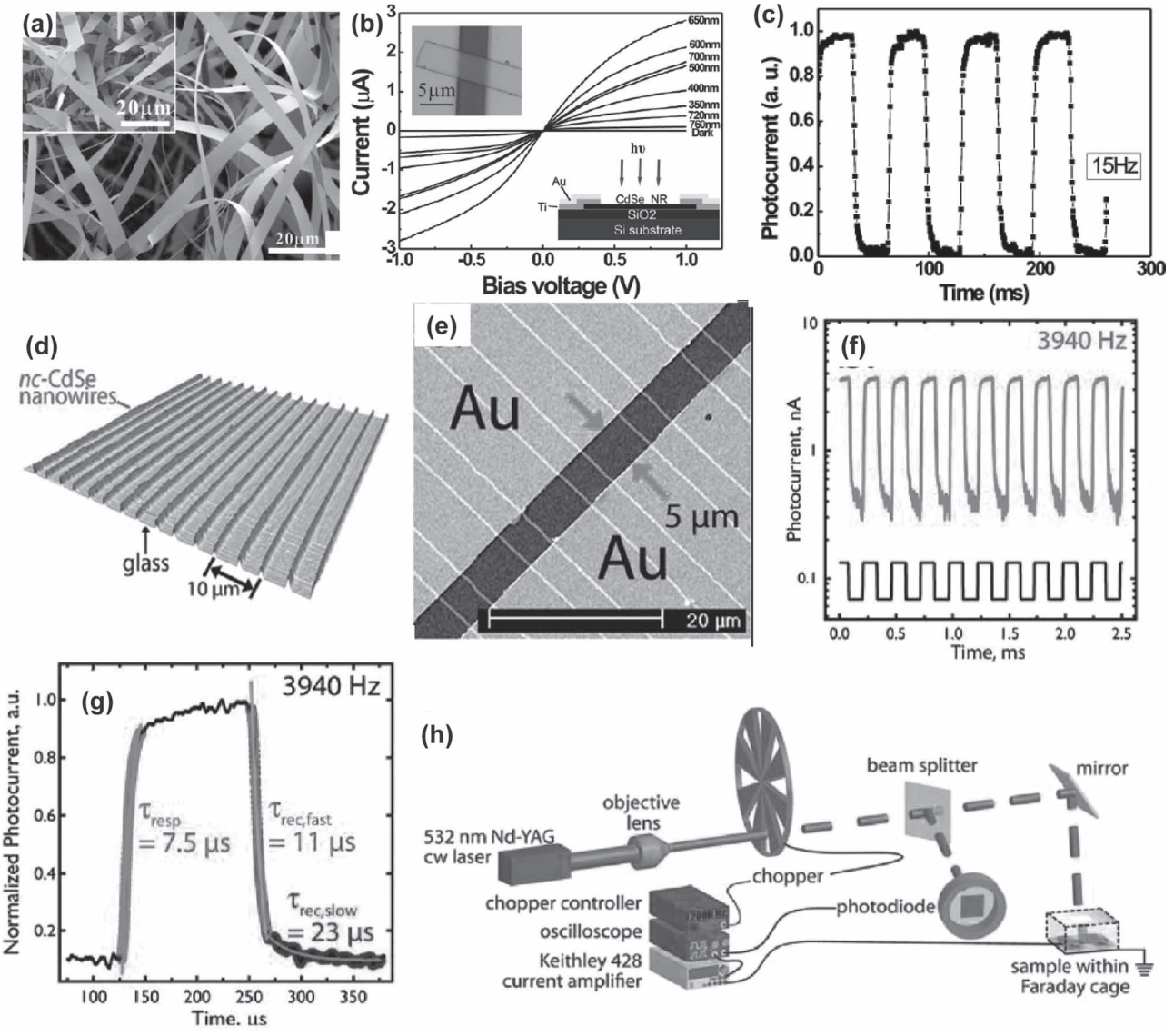

Figure 13. a) SEM images of as-synthesized CdSe nanoribbons. b) *I–V* curves of an individual CdSe nanoribbon illuminated with light of different wavelength. The insets show the optical miscroscopy image of the device (top) and the schematic diagram of the photocurrent measurement (bottom). c) Response characteristics of the photoconductance of CdSe nanoribbon detector to pulses of light irradiation at a frequency of 15 Hz. Reproduced with permission.[53b] d) Atomic force microscopy image of an 80 μm × 80 μm area of an array of nc-CdSe nanowires. e) SEM images showing the 5 μm gap used for the photoconductivity measurements of nc-CdSe nanowire arrays studied; each array contained approximately 350 individual nanowires. f) Modulation of the photocurrent as a function of time in response to chopped illumination (532 nm, 59 mW cm^{-2}) at frequencies of 3940 Hz, nanowires were biased at 2 V, the black trace (shown at bottom) is the current response to the chopped illumination produced by a silicon photodiode. g) Normalized photocurrent versus time showing three exponential fits and the associated time constants for the response (τ_{resp}) and recovery ($\tau_{rec,fast}$ and $\tau_{rec,slow}$) edges. Reproduced with permission.[58] Copyright 2010, American Chemical Society. h) Schematic diagram showing the apparatus used to measure the photoconductivity properties of nc-CdSe nanowires. Reproduced with permission.[59] Copyright 2011, American Chemical Society.

The drain-source current on/off modulation ratio (I_{on}/I_{off}) ratio is typically ≈105 with a maximum of 106, and typical subthreshold slopes are 0.26 V dec^{-1}. Such performance parameters should make these devices attractive for a wide variety of applications.

3.3. Field Emission Properties

Field emission (FE) is based on the physical phenomenon of quantum tunneling, during which electrons are injected from a material's surface into vacuum under the influence of an applied electric field.[65,66] Most recently, Zhai, Jiang, and co-workers developed the FE properties of CdSe nanowires.[67] They designed and synthesized ordered CdSe nanowire branched arrays while merging two particular structural features within a single nanomaterial. **Figure 15**a,b shows the representative SEM images of as-synthesized CdSe products. The ordered high-density CdSe nanowire branched arrays homoepitaxially grow out of the CdSe microrod stems. Figure 15c,d illustrates the FE current density, *J*, as a function of the applied field,

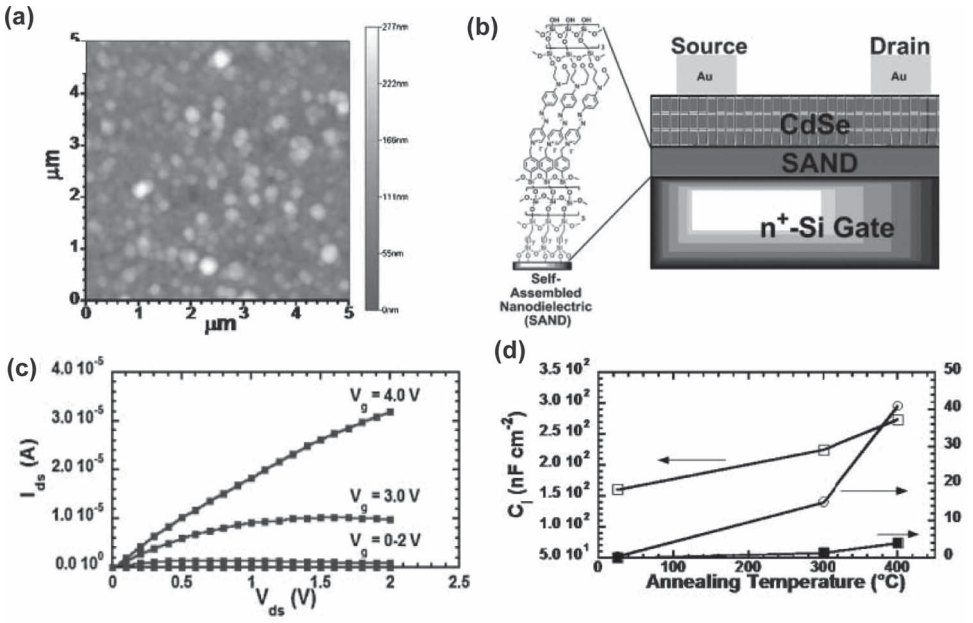

Figure 14. a) AFM image of CBD CdSe films grown on the n^+-Si/SAND substrate and annealed at 400 °C. b) Left: structure of an ≈5.5 nm thick SAND gate insulator composed of alkyl (bottom), siloxane (lower middle and top), and stilbazolium (upper middle) layers. Right: top-contact, bottom-gate FET structure used in this study, fabricated on a n^+-Si gate/substrate, with 3 nm × 5.5 nm SAND multilayers as the gate dielectric, an ≈200nm CdSe film as the semiconductor, and Au source/drain electrodes. c) *I* – *V* output for n^+-Si/SAND/CdSe/Au structured FETs. The FET channel length and width were 100 µm and 500 µm, respectively. d) The capacitance of the film FET versus annealing temperature. Reproduced with permission.[64]

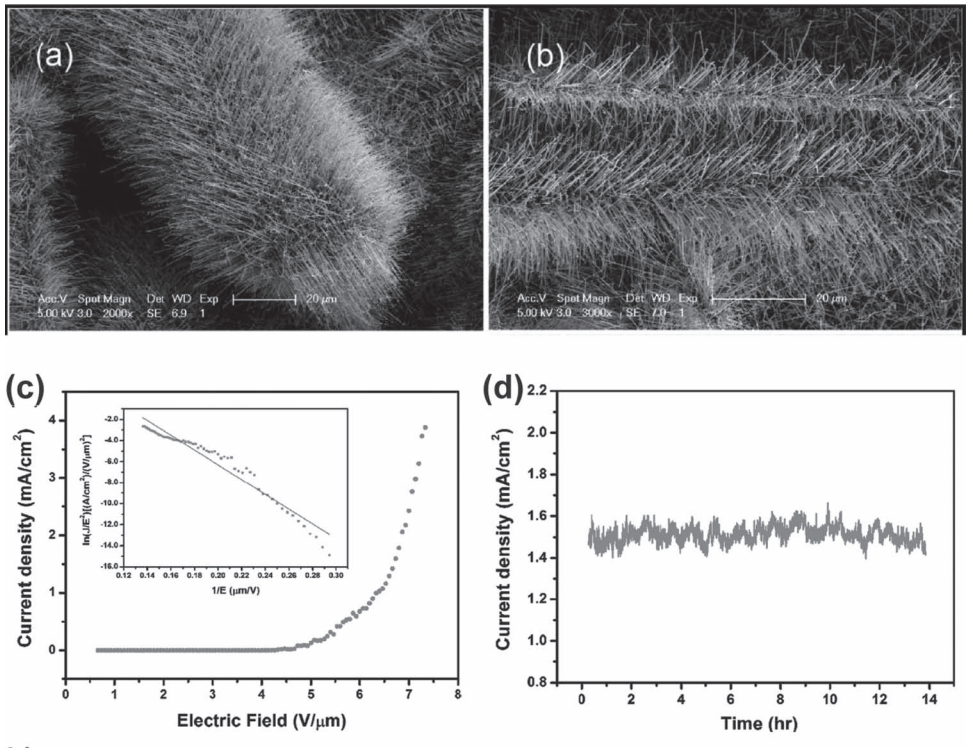

Figure 15. a,b) Typical SEM images of CdSe branched architectures. FE properties of the branched CdSe architectures: c) *J* – *E* curve with a turn-on field of 4.3 ± 0.2 V µm^{-1} and a threshold field of 6.3 ± 0.3 V µm^{-1} for the current densities of 10 and 1 mA cm^{-2}, respectively. The inset is a Fowler–Nordheim (F–N) plot corresponding to (c) and the straight line is a linear fit of the ln(*J*/ E^2) – (1/*E*) plot. d) A stable emission current of the branched CdSe architectures over 14 h. Reproduced with permission.[67] Copyright 2011, American Chemical Society.

E, for a *J*–*E* plot (Figure 15c) and a ln (J/E^2) – ($1/E$) plot (the inset of Figure 15c) at an anode–cathode separation of 150 μm. It is found that the current density exponentially increases with the field increase. The turn-on field at a current density of 10 μA cm^{-2} is 4.3 ± 0.2 V μm^{-1} and the threshold field at a current density of 1.0 mA cm^{-2} is 6.3 ± 0.3 V μm^{-1}, indicating that these CdSe novel nanostructures could potentially be used as excellent field emitters.

3.4. Solar Cells

Solar cells, in which electricity is generated directly from sun light, promise to offer a clean solution to the energy crisis and have attracted considerable interest nowadays. As an important semiconductor material with a suitable bandgap for visible light absorption, CdSe exhibits widespread applications in photovoltaic devices. The application of CdSe in solar cells can be classified into three types:

1) Since its bandgap covers most of the visible spectrum, CdSe can act as carrier transport material for solar cells. For instance, colloidal CdSe and CdTe nanorods were constructed into bilayer nanocrystal solar cells with power conversion efficiencies of 3%.[68] Recently, the solar cells incorporating CdSe and CdS quantum dots have also been studied.[69,70] Kuno and co-workers fabricated solar cells from CdSe nanowires, showing nominal, maximum incident-photon-to-carrier conversion efficiencies (IPCE) values of 13% at 500 nm with associated 1 sun power conversion efficiencies of 0.007% due to the existence of voids between CdSe nanowires. They found that adding colloidal CdSe quantum dots to CdSe nanowire solar cells improves their efficiencies from 13% to 25% at 500 nm. The reason should be attributed to the fact that the CdSe dots, not only fill these voids, but also have similar electron affinities/ionization potentials to nanowires, enabling them to improve transport connectivity within the network.[70]

Most recently, Cao and co-workers have successfully developed novel solar cells by coating carbon nanotube (CNT) films on CdSe nanobelts, respectively.[71] For the CNT-CdSe based solar cells, the CNT film forms junction with CdSe nanobelt in the overlapped area and also serves as a transparent electrode to allow illumination from this side. The excited electron–hole pairs within CdSe under illumination are separated in this junction, where holes are directed to the CNT film and electrons are transported through the nanobelt to the Al electrode (**Figure 16**a). As seen from the band diagram of the CNT/CdSe interface in Figure 16b, the CNT films form a Schottky barrier with the semiconducting CdSe nanobelt in the junction area. An individual CdSe nanobelt serves as a planar substrate for depositing CNT networks and forming the interface for charge separation (Figure 16c). An optical image of a solar cell (Figure 16d) and the corresponding SEM image in Figure 16e show that the filling-fraction of the porous CNT film on the CdSe nanobelt is about 30–40%. The CdSe nanobelt serves as a flat substrate to sustain a network of nanotubes, while the nanotube film forms a Shottky junction with the underlying nanobelt at their interface and also makes a transparent electrode for the device. As shown in Figure 16f,g, this CNT-CdSe junction solar cell has open-circuit voltages of 0.5 to 0.6 V and modest power conversion efficiencies (0.45–0.72%) under AM 1.5 G, 100 mW cm^{-2} light conditions, demonstrating a promising way to develop large-area solar cells based on thin films of CNTs and semiconducting nanostructures. This unique route has been extended to a graphene layer-CdSe nanobelt system for solar cells.[72]

2) Decoration of CdSe semiconductor nanostructures on inorganic compounds. The advantage, with which the bandgap can be tuned by varying particle size, and other inherent absorption properties, makes CdSe a very promising candidate for efficient light-harvesting materials in this type of solar cell. CdSe nanostructures, in particular the CdSe QDs, can function as efficient sensitizers across a broad spectral range from the visible to mid-infrared and offer advantages such as the tunability of optical properties and electronic structure by simple variation in size, while retaining the appeal of low-cost fabrication.[73] In recent years, a lot of work on CdSe-sensitized solar cells has been reported. Typically, by using a CdSe sensitized nanocrystalline TiO_2 photoelectrode in a photoelectrochemical cell, Niitsoo and co-workers achieved a 2.8% conversion efficiency under 1 sun illumination.[74] Using a CdSe- sensitized TiO_2 nanotube array photoelectrode, Peng and co-workers reported an efficiency of 4.15% for an electrochemical cell.[75] Kamat and co-workers fabricated CdSe-sensitized TiO_2 nanorod array solar cells to significantly enhance the photocurrent of the device.[76] For the sandwich structure solar cell, Diguna and co-workers prepared a CdSe sensitized photoelectrode based on a TiO_2 inverse opal and an energy conversion efficiency of 2.7% was obtained.[77] Lo and co-workers sequentially assembled CdS and CdSe quantum dots onto a nanocrystalline TiO_2 film to prepare a CdS/CdSe co-sensitized photoelectrode for solar cell application. An energy conversion efficiency of 4.22% was achieved using a TiO_2/CdS/CdSe/ZnS electrode, under the illumination at one sun (AM 1.5, 100 mW cm^{-2}).[69] Similar CdS/CdSe co-sensitized solar cells have also been reported on CdS/CdSe-sensitized TiO_2 nanotube/nanowire arrays,[78,79] mesoporous TiO_2 films,[80] SnO_2 particle films,[81] and CdS/CdSe sensitized ZrO_2 porous films.[82a] Fuke and co-workers demonstrated that ≈100% internal quantum efficiency of photon-to-electron conversion can be achieved in butylamine-capped CdSe QD-sensitized TiO_2 solar cells by devices utilizing an aqueous Li_2S electrolyte.[82b]

3) Integration of CdSe semiconductor nanostructures into organic conjugated polymers. These hybrids allow the remarkable electronic and optical properties of organic semiconductors to be combined with CdSe, thus presenting great opportunities for unique photophysical, photochemical, and electrochemical properties. Pioneering work on the application of polymer–CdSe composites on solar cells was carried out by Alivisatos and co-workers.[15,68] They recently demonstrated that the use of binary solvent mixtures in which one of the components is a ligand for the CdSe nanorod is effective for controlling the dispersion of CdSe nanorods in a polymer.[83] After combination of CdSe nanorods in a good hole-transporting polymer, poly(3-hexylthiophene) (P3HT), the composited CdSe nanorod-P3HT film results in nanorod-polymer blend solar cells with a high external quantum efficiency of 59% under 0.1 mW cm^{-2} illumination at 450 nm. Wang and co-workers fabricated hybrid thin films of conjugated polymers and CdSe nanoparticles by using a layer-by-layer (LbL) approach driven by covalent coupling

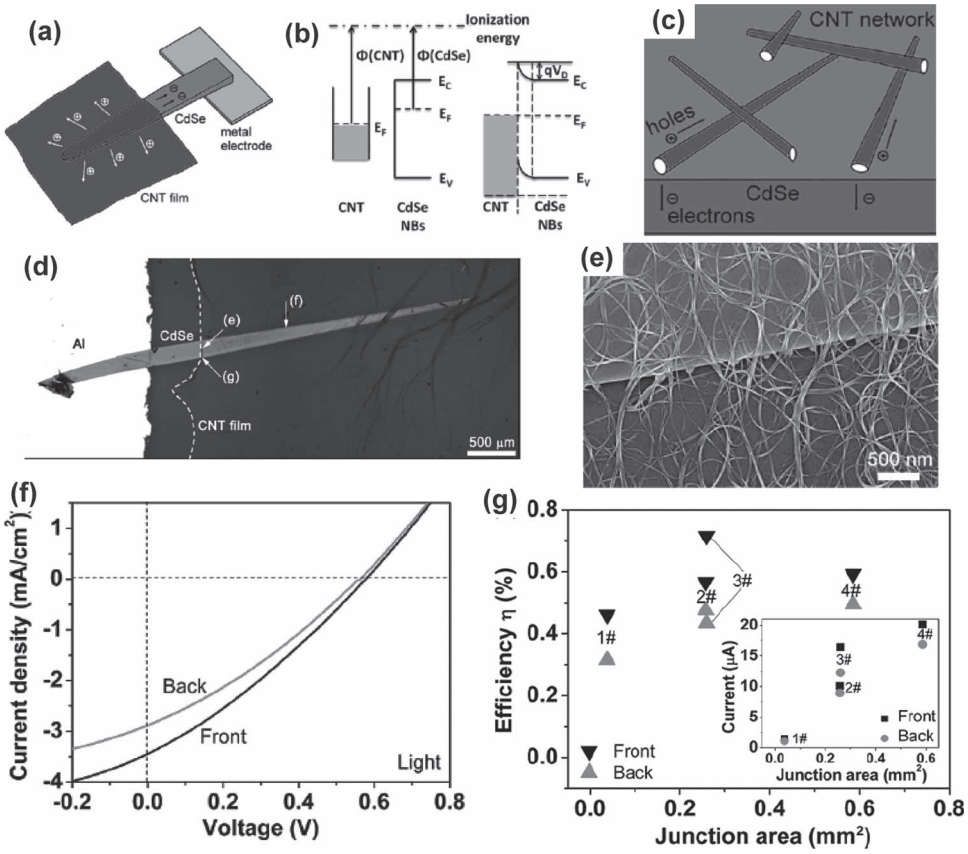

Figure 16. a) Schematic illustration of a nanobelt (deposited on a glass substrate) covered by a CNT film on one end and contacted by an Al electrode on the other end. Arrows show the flow direction of charge carriers (holes and electrons) when the device is illuminated. The overlapped area between the CNT film and the CdSe nanobelt makes the interface for hole–electron separation and acceleration toward different directions. b) The band diagram of the CNT/CdSe interface shows the formation of a Schottky junction at contact. c) Illustration of the interface area between the CNT film and the nanobelt, where holes are directed along the CNT network and electrons are transported through CdSe to the other side. d) Optical image of a CNT-CdSe-Al device consisting of a 3 mm long nanobelt, a transparent CNT film covering about two-thirds of the nanobelt length, and a 100 nm thick Al electrode on the left. e) SEM images of the device showing a highly pure, uniform CNT network coated tightly around the CdSe nanobelt. f) *J–V* curves recorded when the CNT-CdSe junction solar cell is illuminated from the front (CNT film) or back (CdSe nanobelt) side, with open-circuit voltages, V_{oc}, of 0.58 and 0.57 V, short-circuit currents, J_{sc}, of 3.5 and 2.9 mA cm^{-2}, and efficiencies of 0.59 and 0.49%, respectively. g) A summary of cell efficiencies for front and back illumination of the devices with different junction areas. Inset: plot of the photocurrent as a function of CNT-CdSe junction area. Reproduced with permission.[71] Copyright 2010, American Chemical Society.

reactions.[84] A preliminary application of the hybrid films in the development of organic photovoltaics is presented. Upon illumination with white light at 10 mW cm^{-2}, the self-assembled multilayer films exhibit steady photocurrent responses with an overall optical-to-electrical power conversion efficiency of 0.71%.

3.5. Light-Emitting Diodes (LEDs)

In response to ever-increasing energy demands and subsequent costs, a tremendous emphasis is being placed on energy saving, solid-state lighting devices in the form of LEDs. Specifically, a need exists for pure white-light LEDs as a more efficient replacement for conventional lighting sources. High-quality CdSe QDs show high quantum efficiencies and due to the quantum confinement effect their emissions are readily tunable between 500 and 650nm by manipulating their size. Therefore, they have been demonstrated as an ideal material for solid state LEDs. Rosenthal and co-workers demonstrated white-light emission from ultrasmall CdSe nanocrystals.[85,86] These ultrasmall CdSe nanocrystals exhibit broadband emission (420–710 nm) throughout most of the visible light spectrum while not suffering from self absorption. Examples of the white-light emission are shown in **Figure 17**a,b. These properties are the direct result of the extreme surface-to-volume ratio forcing the electron and hole to predominately interact at the CdSe nanocrystal surface. Furthermore, CdSe are good candidates as additional red-emitting components of LEDs. Jeon and co-workers recently synthesized greenish-yellow-emitting Sr_3SiO_5:Ce^{3+}, Li^+, and high-quality TOP/TOPO/HDA-capped CdSe QDs and coated these two luminescent materials onto a blue LED chip to fabricate white LEDs with an excellent color rendering property (as shown in Figure 17c–e).[87] The white LEDs exhibited a luminous efficiency of 14.0 l m W^{-1}, a color rendering index (R_α) of 90.1. The combination of phosphor and QDs in LEDs

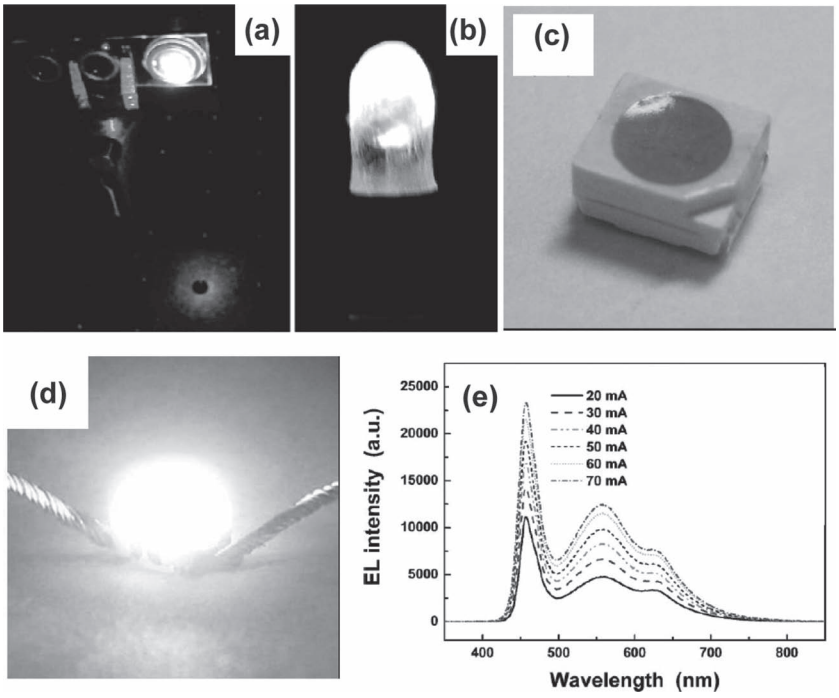

Figure 17. a) White-light emission from magic-sized CdSe. a) Thin film of magic-sized CdSe in polyurethane excited by a frequency doubled titanium:sapphire laser (400 nm) with white light clearly seen reflecting off the table surface. b) A 5 mm commercial UV LED (400 nm) illuminating a thin coating of magic-sized CdSe in polyurethane. Reproduced with permission.[85] Copyright 2005, American Chemical Society. c) Photograph of an as-prepared CdSe QD- and $Sr_3SiO_5:Ce^{3+}$, Li^+, phosphor-based white LED and d) the same white LED operated at 20 mA. e) Electroluminescence spectra of a TOP/TOPO/HDA-capped CdSe QD- and $Sr_3SiO_5:Ce^{3+}$, Li^+ phosphor-based white LED when operated under various forward bias currents. Reproduced with permission.[87]

to obtain light sources with high color rendering properties has also been carried out in CdSe/ZnS core/shell QDs[88] and CdSe/CdS core/shell QDs.[89]

Bawendi and co-workers reported a novel, solid-state CdSe thin-film device that allows for reversible switching of CdSe nanocrystals between charged and uncharged states at room temperature.[90] This device consists of an insulating polymer layer and a thin, spin-coated CdSe nanocrystal layer sandwiched between two electrodes (**Figure 18**a). Reversible fluorescence quenching and absorption bleaching of the CdSe nanocrystal were directly observed, as shown in Figure 18b. There were differences between the charging and discharging process because the number of vacant states for transporting electrons between the CdSe nanocrystals and the electrode during the discharging process is smaller than during the charging process. The drastic changes in the optical properties lead to the potential application of using CdSe nanocrystals in optical modulators and in tunable fluorescent or photochromic displays.

3.6. Memory Devices

Apart from several applications in the optoelectronic devices and FETs summarized above, CdSe have demonstrated applications as electrically bistable devices and memory elements.[91] For example, the devices constructed from thin films of capped CdSe nanoparticles show electrical bistability and have an associated memory phenomenon, confirmed by Pai and co-workers.[92,93] The CdSe nanoparticles were first dispersed in water (**Figure 19**a) and then assembled into monolayer films on a Si wafer using layer-by-layer electrostatic assembly strategy (Figure 19b). The *I–V* characteristics of the monolayer film confirm that the monolayer CdSe nanoparticle films exhibit electrical bistability. The voltage scan towards a negative voltage in a nanoscale regime, as shown in Figure 19c, demonstrates that the CdSe nanoparticles can be used as memory elements with a density of a bit per particle. The time responses of the low- and high-conducting states of a CdSe nanoparticle monolayer in Figure 19d indicate that the nanoparticles retained a state for more than 30 min. This electrical bistabilty can be explained on the basis of charge confinement in the CdSe nanoparticles. Under a suitable negative voltage, the CdSe nanoparticles with higher surface charge density form percolative networks. Such networks finally produce channels across the device resulting in a high-conducting state. The devices based on the CdSe nanoparticles exhibit a high on/off ratio and demonstrate read-only and random-access memory applications. The memory phenomenon has also been found in CdSe/ZnS nanoparticles sandwiched between C-60 layers,[94] CdSe/ZnS nanocrystals in TiO_2 thin films,[95] core/shell CdSe/ZnSe quantum dot/multiwalled carbon nanotube hybrid nanocomposites,[96] CdTe/CdSe core/shell nanoparticles/poly(methylmethacrylate) nanocomposites,[97] and CdSe nanoparticles/poly(methyl methacrylate) (PMMA) blend.[98]

3.7. Biology Applications

CdSe nanocrystals have found applications in biology, mostly as optical imaging agents where the photophysical properties

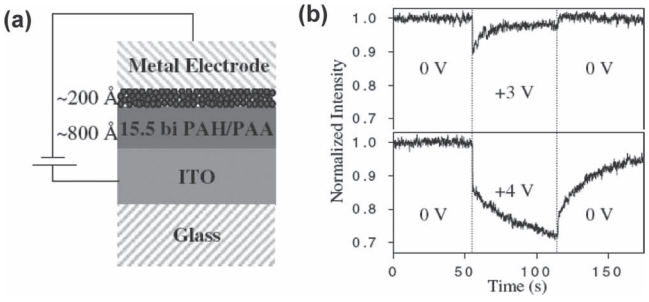

Figure 18. a) Schematic diagram of the CdSe nanocrystal charging device. b) The charging time traces for a bare, 2.2 nm radius, CdSe nanocrystal with 3×10^5 V cm^{-1} (top) and 4×10^5 V cm^{-1} (bottom). Reproduced with permission.[90]

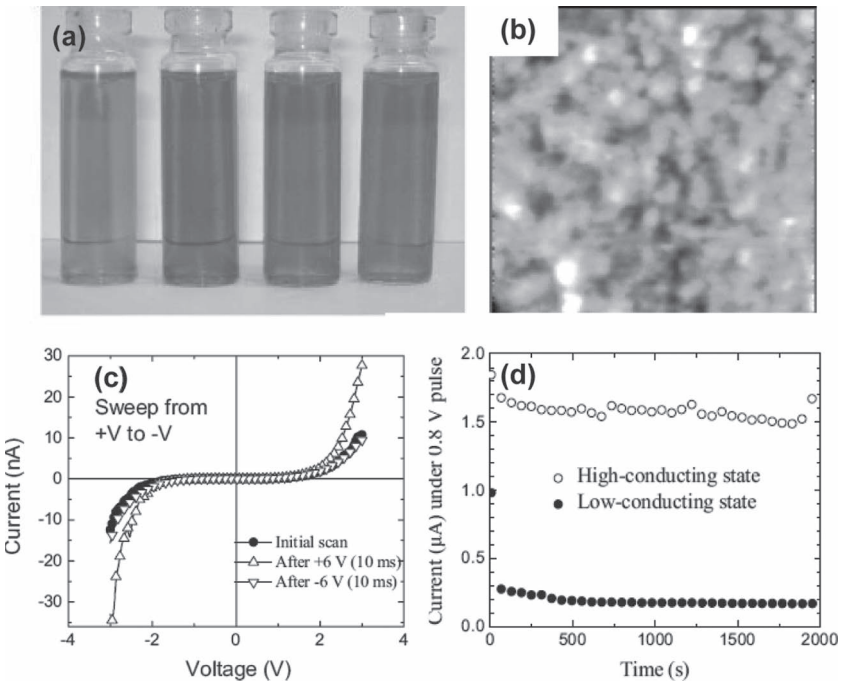

Figure 19. a) Photograph of the solutions dispersed with CdSe nanoparticles of different sizes and b) a monolayer of CdSe nanoparticles showing the presence of nanoparticles on the wafer. c) *I–V* characteristics of the pristine nanoparticle (off state), after switching to a high state (on state), and after reinstating the low-conducting off state. d) Time response of the low- and high-conducting states of a monolayer. Reproduced with permission.[93]

of the nanocrystals are insensitive to species in their environment. The application of CdSe nanocrystal in biosensors has been systematically reviewed by Nocera and co-workers in 2007.[99] Furthermore, Fahmi and co-workers recently reported a simple route to fabricate CdSe nanofibers by self-assembled, elastin-like polymer (ELP)-templated nanoparticles. The CdSe-ELP nanofibers were found to be markedly capable of crossing the cell membrane. These types of nanofibers could be introduced in future medicine nanotechnology and applied in the diagnosis and treatment of various diseases.[100]

4. Conclusions and Outlook

Although the studies of CdSe nanostructures were initiated just a few years ago, the progress is notable and the unique properties and potential applications for electronics, optics, photoelectronics, solar cells, etc. presented reveal that CdSe nanostructures are a promising class of materials. Several morphological CdSe nanostructures including nanoparticles, nanorods, nanowires, nanobelts, nanosheets, nano-tetrapods, and branched nanocrystals have been successfully synthesized through single and combined methods. Hydrothermal/solvothermal techniques, electrochemical deposition processes, CVD and PVD processes, and colloidal methods were highlighted. The hydrothermal/solvothermal technique has the advantages of low cost and simple operation. However the dimensions of the prepared powder products are quite large and the product is highly oxidizable. Electrochemical synthesis, which has the advantages of controlling the shape, size, and growth direction, is a new method for fabricating CdSe nanostructures. The growth is controllable almost exclusively in the direction normal to the substrate surface. However, it is necessary to remove the template for some applications. CVD and PVD processes can synthesize CdSe nanostructures with novel morphologies, but the reaction is poorly controllable and repeatable. The sizes and morphologies of CdSe nanostructures can be readily controlled by the colloidal method, but the precursors used often include organometallic materials and organic solvents, which are highly hazardous and unstable, and it also requires waterless and oxygen-free environments.

Therefore, considerable interest in the future study of fabricating of CdSe nanostructures is proposed. First, new fabrication technologies are still developing for the synthesis of CdSe nanostructures. For example, chemical transformation was used to convert trigonal selenium nanowires into a variety of metal chalcogenide nanostructures, such as Ag_2Se nanowires. Then cation-exchange reaction between Ag^+ and Cd^{2+} was used to transform these single-crystal Ag_2Se nanowires into single-crystal CdSe nanowires.[101,102] Se/CdSe nanocables were synthesized by reacting cadmium salts with Se nanowires, then CdSe nanotubes could be fabricated through thermal evaporation of the Se core nanowires.[103] Second, high emission efficiency from band-edge states of nanocrystals is required if they are to be used as emitters in any application. However, the band-edge emission from nanocrystals has to compete with both radiative and nonradiative decay channels, originating from surface electronic states. In colloidal nanocrystals, coating the surface of the nanocrystals with suitable organic molecules can minimize this problem. The judicious choice of passivating agent can, in fact, improve the size-dependent band-edge luminescence efficiency, while preserving the solubility and processability of the nanocrystals.[104] Unfortunately, passivation by means of organic molecules is often incomplete or reversible, exposing some regions of the surface to degradation effects such as photooxidation.[105,106] In some cases, chemical degradation of the ligand molecule itself or its exchange with other ligands might lead to unstable and therefore unusable nanocrystals.[106] Inorganic core/shell structures can avoid this problem, i.e., an inorganic material can be epitaxially grown on its surface in order to efficiently and permanently remove most of the surface states of the CdSe nanocrystals,[107–115] in analogy with the well-developed techniques for the growth of 2D quantum wells.[116–120] A stringent requirement for the epitaxial growth of several monolayers of one material on the top of another is a low lattice mismatch between the two materials. For example, the lattice of CdS can match well with that of CdSe and thus a CdS monolayer was often used as the shell for CdSe core nanostructures.[47] Third, semiconductor nanostructure arrays

have shown to be of great scientific and technical interest since they have strong non-linear and electro-optic effects that occur due to carrier confinement in three dimensions.[121–125] Considerable efforts have been made with respect to the growth of various semiconductor nanostructure arrays via chemical or physical routes in a controlled way, such as with ZnS nanostructure arrays.[126] However, the relative studies on CdSe nanostructure arrays are limited. Fourth, heterostructures consisting of two or more important functional materials are of prime importance for revealing unique properties and are essential for developing potential nanoscale devices. The fabricating of CdSe nanostructure based heterostructures will be highly valuable for building multifunctional and property-tuning optoelectronic devices, nanogenerators, and solar cells. Fifth, and finally, binding and doping with specific materials have been proven to be facile and effective routes to optimize the device performances. The work to tune the CdSe conductivity, bandgap, surface and optical properties, and so on through a control of the surface functionalization and binding and hybrid with organic nanostructures will also be an important direction.

The nanocrystalline-based solar cell is now emerging as a competitive technology for practical applications due to simple preparation technologies and low costs. CdSe nanocrystals have potential applications in low-cost and high performance hybrid solar cells. In this case, inorganic semiconductor nanocrystals can be used as the electron acceptor in organic-inorganic blends. Such hybrid polymer-inorganic solar cells utilize the high electron mobility of the inorganic phase to overcome charge-transport limitation associated with polymer materials as donor phases with high absorption coefficients. As a result, such a device can combine the advantages of both types of materials: the solution processing of polymer semiconductors and the high charge-carrier mobility of inorganic semiconductors.[83] In the case of CdSe hybrid solar cells, most previous research focused on the rod- or tetrapod-shaped structures synthesized using the method proposed by Peng and co-workers[48] with TOPO as the coordinate surfactant and TOP-Se or TBP-Se as the Se precursor. Although about 95% of the surface ligand TOPO is removed from the CdSe samples by washing the nanocrystals several times with different solvents, the residue TOPO and TOP can still affect the electron transport of the CdSe nanocrystals phase, which will decrease the power conversion efficiency of hybrid solar cells.[127] Therefore, how to thoroughly remove the residual organic ligand and solvent is one of the key requirements for applications in CdSe nanostructure based hybrid solar cells.

In summary, the research activities on the growth of CdSe nanostructures with different morphologies have been comprehensively reviewed. CdSe nanostructures are attractive because of the unique intrinsic characteristics of CdSe materials, the novel physical and chemical properties, and the wide range of potential applications. Research on CdSe nanostructures has shown that there still is a lot of room for future development in this area. It is believed that future research work in this area will further indicate that CdSe nanostructures are powerful functional nanomaterials that will have a major impact on fundamental science research and technological applications.

Acknowledgements

L.J.Z and L.F.H. contributed equally to this work. This work was supported by the National Natural Science Foundation of China (Grant Nos. 91123006, 10904011, 51002032 and 21001028), the National Basic Research Program of China (Grant No. 2012CB932303), Shanghai Chenguang Foundation (11CG06), Shanghai Pujiang Program (11PJ1400300), Science and Technology Commission of Shanghai Municipality (11520706200), and the Programs for Professor of Special Appointment (Eastern Scholar) at Shanghai Institutions of Higher Learning and for New Century Excellent Talents in University (NCET).

Received: December 20, 2011
Published online: February 20, 2012

[1] Cadmium selenide, Wikipedia, The free encyclopedia, http://en.wikipedia.org/wiki/Cadmium_selenide (accessed January 2012).
[2] M. Böhmler, Z. Wang, A. Myalitsin, A. Mews, A. Hartschuh, *Angew. Chem. Int. Ed.* **2011**, *50*, 11536.
[3] T. Ohtsuka, J. Kawamata, Z. Zhu, T. Yao, *Appl. Phys. Lett.* **1994**, *65*, 466.
[4] a) A. P. Alivisatos, *J. Phys. Chem.* **1996**, *100*, 13226; b) X. G. Peng, J. Wickham, A. P. Alivisatos, *J. Am. Chem. Soc.* **1998**, *120*, 5343.
[5] C. B. Murray, D. J. Norris, M. G. Bawendi, *J. Am. Chem. Soc.* **1993**, *115*, 8706.
[6] a) S. L. Ji, L. L. Yin, G. D. Liu, L. D. Zhang, C. H. Ye, *Chem. Commun.* **2009**, 2344; b) X. S. Fang, T. Y. Zhai, U. K. Gautam, L. Li, L. M. Wu, Y. Bando, D. Golberg, *Prog. Mater. Sci.* **2011**, *56*, 175.
[7] a) W. W. Yu, X. G. Peng, *Angew. Chem. Int. Ed.* **2002**, *41*, 2368; b) W. W. Yu, Y. A. Wang, X. G. Peng, *Chem. Mater.* **2003**, *15*, 4300.
[8] V. I. Klimov, *Los Alamos Science* **2003**, *28*, 214.
[9] J. Wang, M. S. Gudiksen, X. Duan, Y. Cui, C. M. Lieber, *Science* **2001**, *293*, 1455.
[10] X. G. Peng, L. Manna, W. D. Yang, J. Wickham, E. Scher, A. Kadavanich, A. P. Alivisatos, *Nature* **2000**, *404*, 59.
[11] J. T. Hu, L. S. Li, W. D. Yang, L. Manna, L. W. Wang, A. P. Alivisatos, *Science* **2001**, *292*, 2060.
[12] T. S. Ahmadi, Z. L. Wang, T. C. Green, A. Henglein, M. A. El-Sayed, *Science* **1996**, *272*, 272.
[13] V. C. Sundar, J. Lee, J. R. Heine, M. G. Bawendi, K. F. Jensen, *Adv. Mater.* **2000**, *12*, 1102.
[14] W. U. Huynh, J. J. Dittmer, A. P. Alivisatos, *Science* **2002**, *295*, 2425.
[15] M. Bruchez Jr., M. Moronne, P. Gin, S. Weiss, A. P. Alivisatos, *Science* **1998**, *281*, 2013.
[16] W. C. W. Chan, S. M. Nie, *Science* **1998**, *281*, 2016.
[17] a) L. E. Brus, *Appl. Phys. A* **1991**, *53*, 465; b) M. A. Kastrer, *Phys. Today* **1993**, *46*, 24; c) Y. Wang, N. Herron, *J. Phys. Chem.* **1991**, *95*, 525.
[18] a) M. G. Bawendi, P. J. Carroll, W. L. Wilson, L. E. Brus, *J. Chem. Phys.* **1992**, *96*, 946; b) I. A. Kudryatsev, *J. Opt. Soc. Am. B* **1993**, *10*, 100.
[19] D. L. Klein, R. Roth, A. K. L. Lim, A. P. Alivisatos, P. McEuen, *Nature* **1997**, *389*, 699.
[20] C. Wang, M. Shim, P. Guyott-Sionnest, *Science* **2001**, *291*, 2390.
[21] W. K. Woo, K. T. Shimizu, M. V. Jarosz, R. G. Neuhauser, C. A. Leatherdale, M. A. Rubner, M. G. Bawendi, *Adv. Mater.* **2002**, *14*, 1068.
[22] D. Xu, X. Shi, G. Guo, L. Gui, Y. Tang, *J. Phys. Chem. B* **2000**, *104*, 5061.
[23] X. C. Jiang, B. Mayers, T. Herricks, Y. N. Xia, *Adv. Mater.* **2003**, *15*, 1740.
[24] E. R. Goldman, E. D. Balighian, H. Mattoussi, M. K. Kuno, J. M. Mauro, P. T. Tran, G. P. Anderson, *J. Am. Chem. Soc.* **2002**, *124*, 6378.

[25] S. H. Yu, J. Yang, Z. H. Han, R. Y. Yang, Y. T. Qian, Y. H. Zhang, *J. Solid State Chem.* **1999**, *147*, 637.
[26] P. M. Petroff, G. Medeiros-Riberio, *MRS Bull.* **1996**, *21*, 54.
[27] D. Bimberg, M. Grundmann, N. N. Ledentsov, *MRS Bull.* **1998**, *23*, 32.
[28] A. D. Yoffe, *Adv. Phys.* **2001**, *50*, 1.
[29] J. Hu, T. W. Odom, C. M. Lieber, *Acc. Chem. Res.* **1999**, *32*, 435.
[30] L. J. Lauhon, M. S. Gudiksen, D. Wang, C. M. Lieber, *Nature* **2002**, *420*, 57.
[31] N. F. Borelli, D. W. J. Smith, *J. Non-Crystal. Solids* **1994**, *180*, 25.
[32] A. Lipovskii, E. Kolobkova, V. Petrikov, I. Kang, A. Olkhovets, T. Krauss, M. Thomas, J. Silcox, F. Wise, Q. Shen, S. Kycia, *Appl. Phys. Lett.* **1997**, *71*, 3406.
[33] G. Demazeau, *J. Mater. Sci.* **2008**, *43*, 2104.
[34] Y. D. Li, H. W. Liao, Y. Fan, L. Q. Li, Y. T. Qian, *Mater. Chem. Phys.* **1999**, *58*, 87.
[35] W. Z. Wang, Y. Geng, P. Yan, F. Y. Liu, Y. Xie, Y. T. Qian, *Inorg. Chem. Commun.* **1999**, *2*, 83.
[36] Q. Peng, Y. J. Dong, Z. X. Demg, X. M. Sun, Y. D. Li, *Inorg. Chem.* **2001**, *40*, 3840.
[37] Y. D. Li, H. W. Liao, Y. Ding, Y. Fan, Y. Zhang, Y. T. Qian, *Inorg. Chem.* **1999**, *38*, 1382.
[38] Q. Peng, Y. J. Dong, Z. X. Demng, Y. D. Li, *Inorg. Chem.* **2002**, *41*, 5249.
[39] Y. Liu, H. Y. Qiu, Y. Xu, D. Wu, M. J. Li, J. X. Jiang, G. Q. Lai, *J. Nanopart. Res.* **2007**, *9*, 745.
[40] a) U. K. Gautam, M. Rajamathi, F. Meldrum, P. Morgand, R. Seshadria, *Chem. Commun.* **2001**, 629; b) T. T Wang, J. L. Wang, Y. C. Zhu, F. Xue, J. Cao, Y. T. Qian, *J. Phys. Chem. Soilds.* **2010**, *71*, 940.
[41] C. R. Martin, *Science* **1994**, *266*, 1961.
[42] C. A. Foss, Jr. Gabor, L. Hornyak, J. A. Stockert, C. R. Martin, *J. Phys. Chem.* **1994**, *98*, 2963.
[43] D. S. Xu, X. S. Shi, G. L. Guo, L. L. Gui, Y. Q. Tang, *J. Phys. Chem. B* **2000**, *104*, 5061.
[44] Y. W. Su, C. S. Wu, C. C. Chen, C. D. Chen, *Adv. Mater.* **2003**, *15*, 49.
[45] a) C. Ma, Y. Ding, D. Moore, X. D. Wang, Z. L. Wang, *J. Am. Chem. Soc.* **2004**, *126*, 708; b) C. Ma, Z. L. Wang, *Adv. Mater.* **2005**, *17*, 2635.
[46] a) R. Venugopal, P. I. Lin, C. C. Liu, Y. T. Chen, *J. Am. Chem. Soc.* **2005**, *127*, 11262; b) Z. Y. Wang, Q. F. Lu, X. S. Fang, X. K. Tian, L. D. Zhang, *Adv. Funct. Mater.* **2006**, *16*, 661; c) Z. Y. Wang, X. S. Fang, Q. F. Lu, C. H. Ye, L. D. Zhang, *Appl. Phys. Lett.* **2006**, *88*, 083102.
[47] L. Manna, E. C. Scher, L. S. Li, A. P. Alivisatos, *J. Am. Chem. Soc.* **2002**, *124*, 7136.
[48] Z. A. Peng, X. G. Peng, *J. Am. Chem. Soc.* **2002**, *124*, 3343.
[49] Q. Pang, L. J. Zhao, Y. Cai, D. P. Nguyen, N. Regnault, N. Wang, S. H. Yang, W. K. Ge, R. Ferreira, G. Bastard, J. N. Wang, *Chem. Mater.* **2005**, *17*, 5263.
[50] H. Yu, J. B. Li, R. A. Loomis, P. C. Gibbons, L. W. Wang, W. E. Buhro, *J. Am. Chem. Soc.* **2003**, *125*, 16168.
[51] M. H. Chen, L. Gao, *Inorg. Chem. Commun.* **2004**, *7*, 673.
[52] a) L. Li, P. Wu, X. S. Fang, T. Y. Zhai, L. Dai, M. Y. Liao, Y. Koide, H. Q. Wang, Y. Bando, D. Golberg, *Adv. Mater.* **2010**, *22*, 3161; b) T. Y. Zhai, L. Li, X. Wang, X. S. Fang, Y. Bando, D. Golberg, *Adv. Funct. Mater.* **2010**, *20*, 4233.
[53] a) J. S. Jie, W. J. Zhang, Y. Jiang, S. T. Lee, *Appl. Phys. Lett.* **2006**, *89*, 133118; b) Y. Jiang, W. J. Zhang, J. S. Jie, X. M. Meng, X. Fan, S. T. Lee, *Adv. Funct. Mater.* **2007**, *17*, 1795.
[54] Z. B. He, J. S. Jie, W. J. Zhang, W. F. Zhang, L. B. Luo, X. Fan, G. D. Yuan, I. Bello, S. T. Lee, *Small* **2009**, *5*, 345.
[55] P. C. Wu, Y. Dai, T. Sun, Y. Ye, H. Meng, X. L. Feng, B. Yu, L. Dai, *ACS Appl. Mater. Interfaces* **2011**, *3*, 1859.
[56] S. Y. Jeong, S. C. Lim, D. J. Bae, Y. H. Lee, H. J. Shin, S.-M. Yoon, J. Y. Choi, O. H. Cha, M. S. Jeong, D. Perello, M. Yun, *Appl. Phys. Lett.* **2008**, *92*, 243103.
[57] E. J. Menke, M. A. Thompson, C. Xiang, L. C. Yang, R. M. Penner, *Nat. Mater.* **2006**, *5*, 914.
[58] S. C. Kung, W. E. van der Veer, F. Yang, K. C. Donavan, R. M. Penner, *Nano. Lett.* **2010**, *10*, 1481.
[59] S. C. Kung, W. D. Xing, W. E. van der Veer, F. Yang, K. C. Donavan, M. Cheng, J. C. Hemminger, R. M. Penner, *ACS Nano* **2011**, *5*, 7627.
[60] B. G. Streetmen, S. K. Banerjee, *Solid State Electronic Devices*, Prentice-Hall, Englewood Cliffs, NJ**2006**, p. 540.
[61] a) J. S. Jie, W. J. Zhang, Y. Jiang, S. T. Lee, *Appl. Phys. Lett.* **2006**, *89*, 133118; b) A. Khandelwal, D. Jena, J. W. Grebinski, K. L. Hull, M. K. Kuno, *J. Electron. Mater.* **2006**, *35*, 170.
[62] a) M. K. Skinner, C. Dwyer, S. Washburn, *Appl. Phys. Lett.* **2008**, *92*, 112105; b) C. Liu, P. C. Wu, T. Sun, L. Dai, Y. Ye, R. Ma, G. G. Qin, *J. Phys. Chem. C* **2009**, *113*, 14478.
[63] Z. B. He, W. J. Zhang, W. F. Zhang, J. S. Jie, L. B. Luo, G. D. Yuan, J. X. Wang, C. M. L. Wu, I. Bello, C. S. Lee, S. T. Lee, *J. Phys. Chem. C* **2010**, *114*, 4663.
[64] P. D. Byrne, A. Facchetti, T. J. Marks, *Adv. Mater.* **2008**, *20*, 2319.
[65] N. S. Xu, S. E. Huq, *Mater. Sci. Eng. R* **2005**, *48*, 47.
[66] X. S. Fang, Y. Bando, C. H. Ye, D. Golberg, *Chem. Commun.* **2007**, 3048.
[67] G. H. Li, T. Y. Zhai, Y. Jiang, Y. Bando, D. Golberg, *J. Phys. Chem. C* **2011**, *115*, 9740.
[68] I. Gur, N. A. Fromer, M. L. Geier, A. P. Alivisatos, *Science* **2005**, *310*, 462.
[69] Y. L. Lee, Y. S. Lo, *Adv. Funct. Mater.* **2009**, *19*, 604.
[70] Y. H. Yu, V. K. Prashant, K. Masaru, *Adv. Funct. Mater.* **2010**, *20*, 1464.
[71] L. H. Zhang, Y. Jia, S. S. Wang, Z. Li, C. Y. Ji, J. Q. Wei, H. W. Zhu, K. L. Wang, D. H. Wu, E. Z. Shi, Y. Fang, A. Y. Cao, *Nano Lett.* **2010**, *10*, 3583.
[72] L. H. Zhang, L. L. Fan, Z. Li, E. Z. Shi, X. M. Li, H. B. Li, C. Y. Ji, Y. Jia, J. Q. Wei, K. L. Wang, H. W. Zhu, D. H. Wu, A. Y. Cao, *Nano Res.* **2011**, *4*, 891.
[73] I. Robel, V. Subramanian, M. Kuno, P. V. Kamat, *J. Am. Chem. Soc.* **2006**, *128*, 2385.
[74] O. Niitsoo, S. K. Sarkar, C. pejux, S. Ruhle, D. Cahen, G. Hodes, *J. Photochem. Photobiol. A* **2006**, *181*, 306.
[75] W. T. Sun, Y. Yu, H. Y. Pan, X. F. Gao, Q. Chen, L. M. Peng, *J. Am. Chem. Soc.* **2008**, *130*, 1124.
[76] J. H. Bang, P. V. Kamat, *Adv. Funct. Mater.* **2010**, *20*, 1970.
[77] L. J. Diguna, Q. Shen, J. Kobayashi, T. Toyoda, *Appl. Phys. Lett.* **2007**, *91*, 023116.
[78] a) S. Q. Huang, Q. X. Zhang, X. M. Huang, X. Z. Guo, M. H. Deng, Y. H. Luo, Q. Shen, T. Toyoda, Q. B. Meng, *Nanotechnology* **2011**, *21*, 375201; b) X. F. Guan, S. Q. Huang, Q. X. Zhang, X. Shen, H. C. Sun, D. M. Li, Y. H. Luo, R. C. Yu, Q. B. Meng, *Nanotechnology* **2011**, *22*, 465402.
[79] M. Li, Y. Liu, H. Wang, H. Shen, W. X. Zhao, H. Huang, C. L. Liang, *J. Appl. Phys.* **2010**, *108*, 094304.
[80] C. F. Chi, P. Chen, Y. L. Lee, I. P. Liu, S. C. Chou, X. L. Zhang, U. Bach, *J. Mater. Chem.* **2011**, *21*, 17534.
[81] M. A. Hossain, J. R. Jennings, Z. Y. Koh, Q. Wang, *ACS Nano* **2011**, *5*, 3172.
[82] a) S. Greenwald, S. Ruhle, M. Shalom, S. Yahav, A. Zaban, *Phys. Chem. Chem. Phys.* **2011**, *13*, 19302; b) N. Fuke, L. B. Hoch, A. Y. Koposov, V. W. Manner, D. J. Werder, A. Fukui, N. Koide, H. Katayama, M. Sykora, *ACS Nano* **2010**, *4*, 6377.
[83] W. U. Huynh, J. J. Dittmer, W. C. Libby, G. L. Whiting, A. P. Alivisatos, *Adv. Funct. Mater.* **2003**, *13*, 73.
[84] Z. Q. Liang, K. L. Dzienis, J. Xu, Q. Wang, *Adv. Funct. Mater.* **2006**, *16*, 542.

[85] M. J. Bowers II, J. R. McBride, S. J. Rosenthal, *J. Am. Chem. Soc.* **2005**, *127*, 15378.
[86] M. A. Schreuder, K. Xiao, I. N. Ivanov, S. M. Weiss, S. J. Rosenthal, *Nano Lett.* **2010**, *10*, 573.
[87] H. S. Jang, H. Yang, S. W. Kim, J. Y. Han, S. G. Lee, D. Y. Jeon, *Adv. Mater.* **2008**, *20*, 2696.
[88] a) A. Rizzo, M. Mazzeo, M. Palumbo, G. Lerario, S. D'Amone, R. Cingolani, G. Gigli, *Adv. Mater.* **2008**, *20*, 1886; b) S. H. Kang, C. K. Kumar, Z. Lee, K. H. Kim, C. Huh, E. T. Kim, *Appl. Phys. Lett.* **2008**, *93*, 191116; c) N. Sedat, D. Hilmi, *Opt. Express* **2008**, *16*, 13961; d) S. Nizamoglu, H. V. Demir, *J. Appl. Phys.* **2009**, *105*, 083112.
[89] a) Z. L. Zhao, J. A. Bardecker, A. M. Munro, M. S. Liu, Y. H. Niu, I. K. Ding, J. D. Luo, B. Q. Chen, A. K. Y. Chen, D. S. Ginger, *Nano Lett.* **2006**, *6*, 463; b) P. T. Jing, J. J. Zheng, Q. H. Zeng, Y. L. Zhang, X. M. Liu, X. Y. Liu, X. G. Kong, J. L. Zhao, *J. Appl. Phys.* **2009**, *105*, 044313.
[90] W. K. Woo, K. T. Shimizu, M. V. Jarosz, R. G. Neuhauser, C. A. Leatherdale, M. A. Rubner, M. G. Bawendi, *Adv. Mater.* **2002**, *14*, 1068.
[91] R. M. Kraus, P. G. Lagoudakis, A. L. Rogach, D. V. Talapin, H. Weller, J. M. Lupton, J. Feldmann, *Phys. Rev. Lett.* **2007**, *98*, 017401.
[92] S. Sahu, S. K. Majee, A. J. Pai, *Appl. Phys. Lett.* **2007**, *91*, 143108.
[93] B. C. Das, S. K. Batabyal, A. J. Pai, *Adv. Mater.* **2007**, *19*, 4172.
[94] F. Li, D. I. Son, J. H. Ham, B. J. Kim, J. H. Jung, T. W. Kim, *Appl. Phys. Lett.* **2007**, *91*, 162109.
[95] S. H. Kang, C. K. Kumar, Z. Lee, V. Radmilovic, E. T. Kim, *Appl. Phys. Lett.* **2009**, *95*, 183111.
[96] F. S. Li, D. I. Son, T. W. Tae, E. Ryu, S. W. Kim, *Nanotechnology* **2009**, *20*, 085202.
[97] D. Y. Yun, J. M. Son, T. W. Kim, S. W. Kim, S. W. Kim, *Appl. Phys. Lett.* **2011**, *98*, 243306.
[98] J. M. Kim, D. H. Lee, T. S. Yoon, H. H. Lee, J. W. Lee, Y. S. Kim, *Electrochem. Solid-State Lett.* **2011**, *14*, H238.
[99] R. C. Somers, M. G. Bawendi, D. G. Nocera, *Chem. Soc. Rev.* **2007**, *36*, 579.
[100] A. Fahmi, T. Pietsh, M. Bryszewska, J. Carlos, R. Cabello, A. K. Chyla, F. J. Arias, M. A. Rodrigo, N. Gindy, *Adv. Funct. Mater.* **2010**, *20*, 1011.
[101] U. Y. Jeong, Y. N. Xia, Y. D. Yin, *Chem. Phys. Lett.* **2005**, *416*, 246.
[102] U. Y. Jeong, P. H. C. Camargo, Y. H. Lee, Y. N. Xia, *J. Mater. Chem.* **2006**, *16*, 3893.
[103] X. Jiang, B. Mayers, T. Herricks, Y. N. Xia, *Adv. Mater.* **2003**, *15*, 1740.
[104] D. V. Talapin, A. L. Rogach, A. Kornowski, M. Haase, H. Weller, *Nano Lett.* **2001**, *1*, 207.
[105] J. E. B. Katari, V. L. Colvin, A. P. Alivisatos, *J. Phys. Chem.* **1994**, *98*, 4109.
[106] J. Aldana, Y. A. Wang, X. G. Peng, *J. Am. Chem. Soc.* **2001**, *123*, 8844.
[107] L. Spanhel, M. Haase, H. Weller, A. Henglein, *J. Am. Chem. Soc.* **1987**, *109*, 5649.
[108] C. F. Hoener, K. A. Allan, A. J. Bard, A. Campion, M. A. Fox, T. E. Mallouk, S. E. Webber, J. M. White, *J. Phys. Chem.* **1992**, *96*, 3812.
[109] A. Eychmuller, A. Mews, H. Weller, *Chem. Phys. Lett.* **1993**, *208*, 59.
[110] M. A. Hines, P. Guyot-Sionnest, *J. Phys. Chem.* **1996**, *100*, 468.
[111] B. O. Dabbousi, J. Rodriguez Viejo, F. V. Mikulec, J. R. Heine, H. Mattoussi, R. Ober, K. F. Jensen, M. G. Bawendi, *J. Phys. Chem. B* **1997**, *101*, 9463.
[112] X. G. Peng, M. C. Schlamp, A. V. Kadavanich, A. P. Alivisatos, *J. Am. Chem. Soc.* **1997**, *119*, 7019.
[113] S. V. Kershaw, M. Burt, M. Harrison, A. Rogach, H. Weller, A. Eychmuller, *Appl. Phys. Lett.* **1999**, *75*, 1694.
[114] Y. W. Cao, U. Banin, *J. Am. Chem. Soc.* **2000**, *122*, 9692.
[115] S. Haubold, M. Haase, A. Kornowski, H. Weller, *ChemPhysChem* **2001**, *2*, 331.
[116] M. A. Herman, H. Sitter, *Microelectron. J.* **1996**, *27*, 257.
[117] R. Beanland, D. J. Dunstan, P. J. Goodhew, *Adv. Phys.* **1996**, *45*, 87.
[118] D. J. Dunstan, *J. Mater. Sci.: Mater. Electron.* **1997**, *8*, 337.
[119] N. N. Ledentsov, V. M. Ustinov, V. A. Shchukin, P. S. Kop'ev, Z. I. Alferov, D. Bimberg, *Semiconductors* **1998**, *32*, 343.
[120] V. A. Shchukin, D. Bimberg, *Rev. Mod. Phys.* **1999**, *71*, 1125.
[121] Y. Li, G. W. Meng, L. D. Zhang, F. Phillipp, *Appl. Phys. Lett.* **2000**, *76*, 2011.
[122] B. Das, S. P. McGinnis, *Appl. Phys. A* **2000**, *71*, 681.
[123] X. S. Fang, L. F. Hu, K. F. Huo, B. Gao, L. J. Zhao, M. Y. Liao, P. K. Chu, Y. Bando, D. Golberg, *Adv. Funct. Mater.* **2011**, *21*, 3907.
[124] Z. Zhang, T. Shimizu, L. J. Chen, S. Senz, U. Goesele, *Adv. Mater.* **2009**, *21*, 4701.
[125] H. Yoon, K. Seo, N. Bagkar, J. In, J. Park, J. Kim, B. Kim, *Adv. Mater.* **2009**, *21*, 4979.
[126] X. S. Fang, L. M. Wu, L. F. Hu, *Adv. Mater.* **2011**, *23*, 585.
[127] L. L. Han, D. H. Qin, X. Jiang, Y. S. Liu, L. Wang, J. W. Chen, Y. Cao, *Nanotechnology* **2006**, *17*, 4736.